

Freed-Isobar Analysis of Light Mesons at COMPASS

F. Krinner* for the COMPASS collaboration

*Max Planck Institut for Physics,
80805 Munich, Bavaria, Germany*

**E-mail: fkrinner@mpp.mpg.de*

Modern hadron-spectroscopy experiments such as COMPASS collect data samples of unprecedented size, so that novel analysis techniques become possible and necessary. One such technique is the freed-isobar partial-wave analysis (PWA). In this approach, fixed parametrizations for the amplitudes of intermediate states commonly modeled using Breit-Wigner shapes are replaced by sets of step-like functions that are determined from the data. This approach not only reduces the model dependence of partial-wave analyses, but also allows us to study the amplitudes of the intermediate states and their dependence on the parent system.

We will also present results of a freed-isobar PWA performed on the large data set on diffractive production of three charged pions collected by the COMPASS experiment, which consists of 46×10^6 exclusive events. We will focus on results for the wave with spin-exotic quantum numbers $J^{PC} = 1^{-+}$, in particular on its decay into $\rho(770)\pi$. Here, the freed-isobar PWA method provides insight into the interplay of three- and two-particle dynamics and confirms the decay of the spin-exotic $\pi_1(1600)$ resonance to $\rho(770)\pi$ in a model-independent way.

Keywords: Exotic; model independent; partial-wave analysis; PWA; freed-isobar.

1. Diffractive 3π production

The data set presented here was collected in 2008 by the COMPASS experiment located at CERN's North Area using a $190 \text{ GeV}/c \pi^-$ beam impinging on liquid hydrogen serving as a proton target. Using the two-stage COMPASS spectrometer, the process

$$\pi_{\text{beam}}^- + p_{\text{target}} \rightarrow \pi^- \pi^+ \pi^- + p_{\text{recoil}} \quad (1)$$

is selected resulting in a sample of 46×10^6 exclusive events. These events have been analyzed in an extensive PWA¹ and the resonance parameters of eleven isovector 3π resonances have been extracted².

2. Freed-isobar PWA method

The measured intensity distribution $\mathcal{I}(\vec{\tau})$ for a given $m_{3\pi}$ and t' bin is a function of the five phase space variables $\vec{\tau}$ and is modeled as the modulus square of a coherent sum over partial-wave amplitudes:

$$\mathcal{I}(\vec{\tau}) = \left| \sum_{\text{waves}} \mathcal{T}_{\text{wave}} \mathcal{A}_{\text{wave}}(\vec{\tau}) \right|^2. \quad (2)$$

Here, the complex-valued transition amplitudes $\mathcal{T}_{\text{wave}}$ encode the strengths and phases with which single partial waves contribute and the decay amplitudes $\mathcal{A}_{\text{wave}}(\vec{\tau})$ describe the 3π decay and encode the $\vec{\tau}$ -dependence of the partial waves.

The conventional PWA model uses a set of 88 partial waves that differ in spin quantum numbers and 2π resonance content¹. The decay amplitudes are split up under the assumption that production and decay of appearing 2π and 3π resonances factorize and the process can therefore be described as two subsequent two-particle decays. This assumption is known as the isobar model:

$$\mathcal{A}_{\text{wave}}(\vec{\tau}) = \psi_{\text{wave}}(\vec{\tau}) \Delta_{\text{wave}}(m_{\pi\pi}) + \text{Bose symm.}, \quad (3)$$

where $\psi_{\text{wave}}(\vec{\tau})$ describes the dependence of the partial wave on the decay angles which is fully determined from first principles by the appearing spin quantum numbers. The dynamic isobar amplitudes $\Delta_{\text{wave}}(m_{\pi\pi})$ in contrast describe the 2π resonance content—or isobar—of the partial waves and have to be known beforehand. Bose symmetrization is necessary due to the two identical final-state π^- .

The choice of 2π resonance content, its parameterizations and its parameters introduces possible model bias to the partial wave model and neglects possible contributions from low-intensity resonances or final-state interactions of the isobar with the third pion. To overcome this, we re-analyzed the data set using the freed-isobar approach, in which we replace the fixed dynamic isobar amplitudes by sets of indicator functions spanning the kinematically allowed $m_{\pi\pi}$ range:

$$\Delta_{\text{wave}}(m_{\pi\pi}) \rightarrow \sum_{\text{bins}} \Delta_{\text{wave}}^{\text{bin}}(m_{\pi\pi}) \quad \text{with} \quad \Delta_{\text{wave}}^{\text{bin}}(m_{\pi\pi}) = \begin{cases} 1 & m_{\pi\pi} \in \text{bin}, \\ 0 & \text{otherwise.} \end{cases} \quad (4)$$

This replacement alleviates the necessity for fixed dynamic isobar amplitudes from the partial wave model, resulting in a much higher number of

parameters, that can lead to mathematical ambiguities within the model—so-called zero modes—that have to be identified and resolved. The detailed origin of these ambiguities in general and for the data presented here is discussed in Refs. [3–5].

We replaced the dynamic isobar parameterizations of 12 of the 88 waves in the PWA model of Ref. [1] following eq. 4. Eleven of these waves represent the waves describing the largest intensities in the model, so that 75% of the total intensity is described by the freed waves. This minimizes possible effects of imperfections in the fixed isobar parameterizations of the remaining waves. The twelfth wave is the spin-exotic $1^{-+}1^{+}[\pi\pi]_{1--}\pi\text{P}$ wave^a, which will be presented in Sec. 3. We use an $m_{\pi\pi}$ bin width of $40\text{ MeV}/c^2$, and a region of narrower bins of $20\text{ MeV}/c^2$ around the $\rho(770)$ resonance. The analysis was performed in 50 equidistant bins in the mass range $0.5 < m_{3\pi} < 2.5\text{ GeV}/c^2$ and four non-equidistant bins in the squared four-momentum transfer t' , resulting in 200 independently fitted kinematic cells.

3. Results for the spin-exotic wave

The result of this analysis is shown in Fig. 2. As expected, the resulting two-dimensional intensity distribution on the right side is dominated by a clear peak corresponding to the decay $\pi_1(1600) \rightarrow \rho(770)\pi$. This confirms the existence of this decay without any assumption on the dynamic amplitude of the $[\pi\pi]_{1--}$ system. The left plot shows the coherent sum of all $m_{\pi\pi}$ bins, compared to the result from the conventional PWA. Both distributions are dominated by a similar peak corresponding to the $\pi_1(1600)$ resonance. The freed-isobar result has a higher over-all intensity, since it also can pick up intensity away from the $\rho(770)$ peak.

Fig. 1 shows the results of the analysis of the data in the highest t' bin for three $m_{3\pi}$ bins, below, on, and above the nominal mass of the $\pi_1(1600)$ resonance. The left column shows the resulting intensity distributions and the right column shows the same data as Argand diagrams. In all three $m_{3\pi}$ bins, the fixed Breit-Wigner amplitude from the conventional PWA agrees nicely with the result of the freed-isobar analysis.

The intensity distribution assumes its highest value in the $m_{3\pi}$ at the $\pi_1(1600)$ mass and the Argand diagrams rotate counter-clockwise moving

^aThe wave name is given by $J_{3\pi}^{PC} M^\epsilon [\pi\pi]_{J_{\pi\pi}^{PC}} \pi\text{L}$, where J^{PC} are the quantum number of the 3π and $\pi\pi$ systems, M^ϵ is the spin-projection and reflectivity quantum number of the 3π system and L is the orbital angular between the $\pi\pi$ system and the third pion.

4

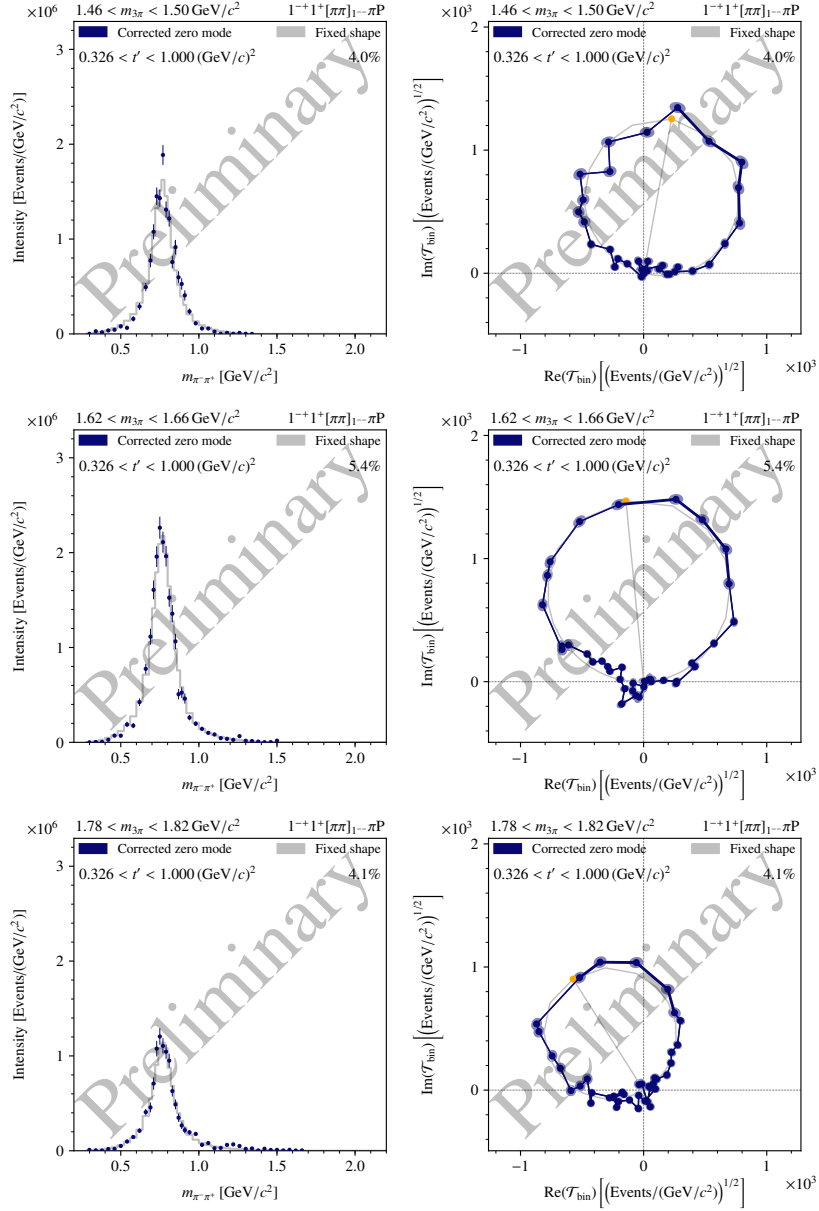


Fig. 1. Results of the freed-isobar PWA for three $m_{3\pi}$ bins (rows) in the highest t' bin for the $1^{-+}1^{+}[\pi\pi]_{1--}\pi P$ wave (blue). The Breit-Wigner amplitude for the $\rho(770)$ as used in the conventional PWA is overlaid in gray. Left: Intensity distributions. Right: Argand diagrams; the orange dot indicates the nominal resonance position of the gray curve.

through the $\pi_1(1600)$ resonance, which both reflects the dynamic amplitude of the $\pi_1(1600)$ mother resonance, which further confirms its existence.

Since the fixed Breit-Wigner amplitude is adequate for all $m_{3\pi}$ slices in Fig. 1, we show two additional bins in Fig. 3 where the shapes do not match equally well. At low $m_{3\pi}$ the dynamic isobar amplitude, exhibits a sharper peak than the fixed Breit-Wigner, i.e. a slightly deformed Argand circle. At high $m_{3\pi}$, it exhibits a second peak in the intensity spectrum at a two-pion mass of $1.6 \text{ GeV}/c^2$, which could correspond to an excited ρ' and is unaccounted for in the conventional approach. Whether this peak actually stems from a resonance, requires a subsequent resonance-model fit.

4. Conclusion

We showed results for the dynamic isobar amplitudes of the spin-exotic $1^{-+}1^+[\pi\pi]_{1--}\pi\text{P}$ wave extracted from COMPASS data on diffractively produced 3π using the freed-isobar approach³⁻⁵. The extracted dynamic isobar amplitudes are in general in agreement with the assumption of a dominant presence of the $\rho(770)$ resonance in the $\pi\pi$ P-wave wave as assumed in the conventional PWA approach¹. In addition, the $\pi_1(1600)$ is confirmed to appear in this partial wave. Nevertheless, there are deviations from the Breit-Wigner amplitude that may originate from distortions of the dynamic isobar amplitude due to non-resonant contributions, such as the Deck effect⁶ or re-scattering effects, or additional excited isobar resonances. To clarify the origin of these deviations, a resonance-model fit to the presented data is work in progress.

References

1. C. Adolph *et al.*, Resonance Production and $\pi\pi$ S-wave in $\pi^- + p \rightarrow \pi^- \pi^- \pi^+ + p_{\text{recoil}}$ at $190 \text{ GeV}/c$, *Phys. Rev.* **D95**, p. 032004 (2017).
2. M. Aghasyan *et al.*, Light isovector resonances in $\pi^- p \rightarrow \pi^- \pi^- \pi^+ p$ at $190 \text{ GeV}/c$, *Phys. Rev.* **D98**, p. 092003 (2018).
3. F. Krinner, D. Greenwald, D. Ryabchikov, B. Grube and S. Paul, Ambiguities in model-independent partial-wave analysis, *Phys. Rev.* **D97**, p. 114008 (2018).
4. F. Krinner, Recent progress in the partial-wave analysis of the diffractively produced $\pi^- \pi^+ \pi^-$ final state at COMPASS, *EPJ Web Conf.* **199**, p. 02003 (2019).
5. F. Krinner, Freed-Isobar Partial-Wave Analysis, PhD thesis, Technische Universität München (2018).
6. R. T. Deck, Kinematical interpretation of the first $\pi-\rho$ resonance, *Phys. Rev. Lett.* **13**, p. 169 (1964).

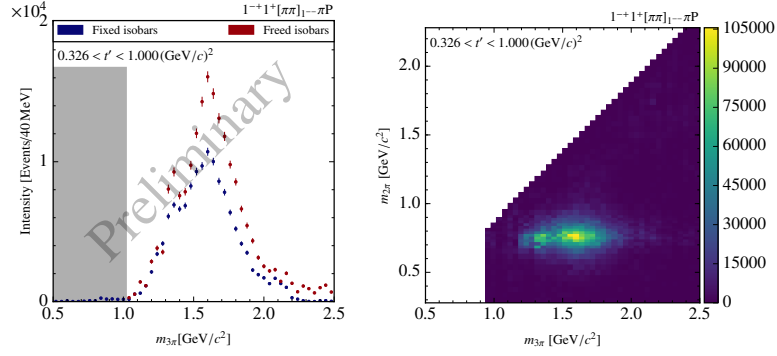


Fig. 2. Results of the freed-isobar analysis for the $1^{-+}1^{+}[\pi\pi]_{1--}\pi P$ wave in the highest t' bin. Left: coherent sum over all $m_{\pi\pi}$ bins (red) compared to the corresponding result of the conventional PWA (blue). Right: Two-dimensional intensity distribution as function of $m_{3\pi}$ and $m_{\pi\pi}$.

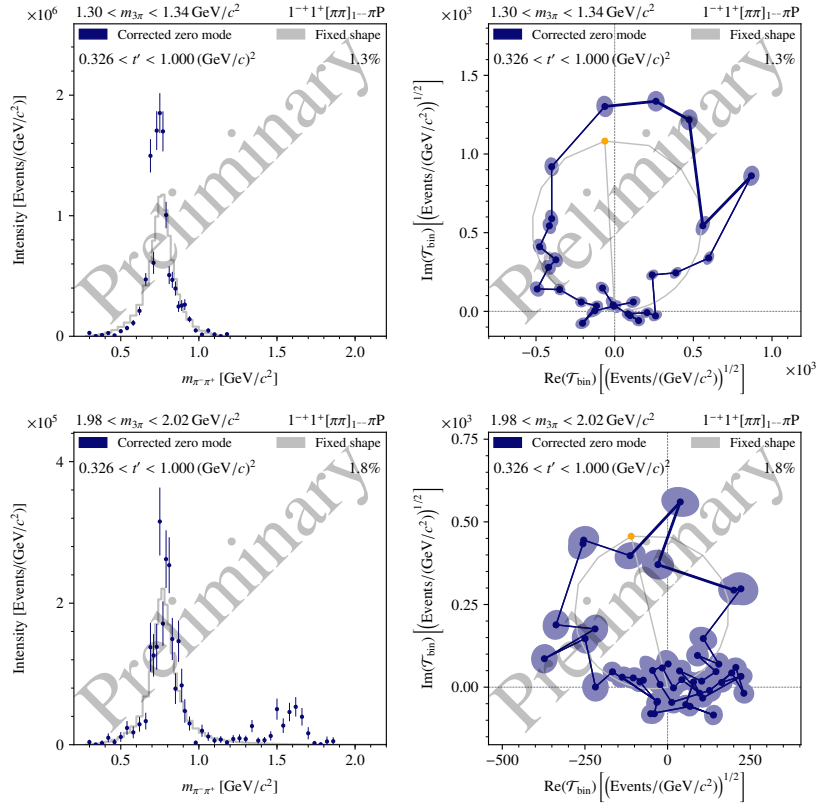


Fig. 3. As Fig. 1 for two additional $m_{3\pi}$ bins far away from the $\pi_1(1600)$ region.